Geophysical Research Letters

RESEARCH LETTER
10.1029/2021GL095560

Special Section:
The COVID-19 pandemic: linking health, society and environment

Measurements of Volatile Organic Compounds During the COVID-19 Lockdown in Changzhou, China

Andrew Jensen[1,2], Zhiqiang Liu[3,4], Wen Tan[5], Barbara Dix[1], Tianshu Chen[1,6], Abigail Koss[5], Liang Zhu[5], Li Li[3], and Joost de Gouw[1,2]

[1]Cooperative Institute for Research in Environmental Sciences, University of Colorado, Boulder, CO, USA, [2]Department of Chemistry, University of Colorado, Boulder, CO, USA, [3]School of Environmental and Chemical Engineering, Shanghai University, Shanghai, China, [4]Changzhou Institute of Environmental Science, Changzhou, China, [5]Tofwerk AG, Thun, Switzerland, [6]Environment Research Institute, Shandong University, Qingdao, China

Abstract The COVID-19 outbreak in 2020 prompted strict lockdowns, reduced human activity, and reduced emissions of air pollutants. We measured volatile organic compounds (VOCs) using a proton-transfer-reaction mass spectrometry instrument in Changzhou, China from 8 January through 27 March, including periods of pre-lockdown, strict measures (level 1), and more relaxed measures (level 2). We analyze the data using positive matrix factorization and resolve four factors: textile industrial emissions (62 ± 10% average reduction during level 1 relative to pre-lockdown), pharmaceutical industrial emissions (40 ± 20%), traffic emissions (71 ± 10%), and secondary chemistry (20 ± 20%). The two industrial sources showed different responses to the lockdown, so emissions from the industrial sector should not be scaled uniformly. The quantified changes in VOCs due to the lockdowns constrain emission inventories and inform chemistry-transport models, particularly for sectors where activity data are sparse, as the effects of lockdowns on air quality are explored.

Plain Language Summary In response to the outbreak of COVID-19 in early 2020 and in the interest of public health, many countries enacted lockdowns. Restrictions on non-essential travel and work resulted in reductions in air pollutant emissions. Concentrations of organic air pollutants were measured in Changzhou, China before and during the lockdowns. These pollutants were then grouped together based on their behavior in time and chemical signatures, and these groups were assigned to emission sources such as motor vehicles and industries. Motor vehicle pollutant emissions were reduced by 70% during the lockdown while textile and pharmaceutical industrial emissions were reduced by 40% and 60%, respectively. Different kinds of industries, such as those that are essential versus non-essential during a global pandemic, responded differently to the lockdown, so industries should not be treated as a single entity. These results inform further studies by providing details on the effect of lockdown on emission sources.

Key Points:

- We measured and quantified volatile organic compounds (VOCs) in Changzhou, China during the COVID-19 lockdowns
- Traffic-related VOC emissions were reduced by 70%, which agrees with reductions in traffic counts
- Textile and pharmaceutical industry VOC emissions responded differently, so industrial emissions should not be scaled uniformly

Supporting Information:

Supporting Information may be found in the online version of this article.

Correspondence to:

L. Zhu and J. de Gouw,
zhu@tofwerk.com;
Joost.deGouw@colorado.edu

Citation:

Jensen, A., Liu, Z., Tan, W., Dix, B., Chen, T., Koss, A., et al. (2021). Measurements of volatile organic compounds during the COVID-19 lockdown in Changzhou, China. *Geophysical Research Letters*, *48*, e2021GL095560. https://doi.org/10.1029/2021GL095560

Received 3 AUG 2021
Accepted 29 SEP 2021

1. Introduction

To contain the spread of coronavirus disease (COVID-19), many countries underwent large-scale lockdowns in 2020. Decreases in vehicle traffic, industrial activity, and power consumption led to reduced emissions of air pollutants and greenhouse gases. For example, reductions in nitrogen dioxide columns were detected over Asia, Europe and North America by space-based instruments (Bauwens et al., 2020; Ding et al., 2020; Goldberg et al., 2020; Liu et al., 2020). Ground-based measurements were used to quantify reductions in emissions in many different regions (Li et al., 2020; Mahato et al., 2020; Singh & Chauhan, 2020; Tanzer-Gruener et al., 2020). Activity data (e.g., energy consumption) have been used to estimate day-by-day emissions from corresponding sectors in European countries (Guevara et al., 2021). These reductions in emissions have attracted attention from the global atmospheric research community as they provide (a) constraints on the scientific understanding of pollutant emissions, and (b) test cases to study the formation of secondary pollutants such as ozone and $PM_{2.5}$ under lower emission conditions (Diffenbaugh et al., 2020; Gkatzelis et al., 2021; Kroll et al., 2020). Initial studies have highlighted the complexity of these issues as emissions reductions did not necessarily lead to lower secondary pollutants in China (Chang et al., 2020; Huang et al., 2021; Le et al., 2020; Shi & Brasseur, 2020; Wang, Chen, et al., 2020).

Research activities were heavily curtailed by the COVID-19 lockdowns. Many studies focused therefore on the analysis of data from satellite instruments and automated air quality monitors of criteria pollutants. Measurements of volatile organic compounds (VOCs), especially highly time-resolved measurements, are generally much sparser and could not be easily expanded during the lockdowns. This limits our understanding of how VOC emissions changed and how the formation of ozone and $PM_{2.5}$ was affected. The changes in VOC emissions from motor vehicles can be estimated with some confidence from the changes in activity data, and in nitrogen oxide (NOx) and carbon monoxide (CO) emissions. However, VOC emissions from motor vehicles have been significantly reduced over past decades and other, evaporative sources from industry and volatile chemical products are more important for ozone (O_3) and organic $PM_{2.5}$ formation in many urban atmospheres (McDonald et al., 2018). The changes in evaporative VOC emissions during the lockdowns cannot be easily estimated other than by measurements.

Here, we analyze VOC measurements made in 2020 from January 8 through March 27 by proton-transfer-reaction time-of-flight mass spectrometry in Changzhou, a Chinese city in the Yangtze River Delta. The data yield detailed insights into the quantitative and compositional changes in regional VOC emissions during the COVID-19 lockdowns. We analyze the data set using positive matrix factorization to separate VOC sources, and describe how different emission sectors were affected. To provide perspective to the VOC data, we also analyzed the results from concurrent measurements of criteria pollutants in Changzhou and from TROPOspheric Monitoring Instrument measurements of nitrogen dioxide (NO_2).

2. Measurements

Changzhou is in the Jiangsu Province on the Yangtze River with a population of approximately 4.5 million. It has a humid, subtropical climate, is part of a metropolitan region between Shanghai and Nanjing (Figure S1 in Supporting Information S1) with many different industries (Li et al., 2021). VOCs were measured from 8 January through 27 March 2020 at the Changzhou Environmental Monitoring Center (CEMC); 31.76 N, 119.96 E in the Tianning District.

Exact dates of lockdown measures varied across China. In this work, we adopt the same periods as defined in a study of the Yangtze River Delta (Li et al., 2020): (a) a pre-lockdown period from 1–23 January, (b) a level 1 response period from 24 January–25 February with the most severe quarantines, (c) a level 2 response period from 26 February–31 March with some resumption of work, and (d) a post-lockdown period starting on 1 April.

Measurements of VOCs were made using a compact Vocus proton-transfer-reaction time-of-flight mass spectrometer (Vocus Elf; Tofwerk AG). VOCs are ionized by reactions with H_3O^+ ions from a discharge and the product ions are detected using a compact time-of-flight mass analyzer (m/Δm FWHM of 950 at *m/Q* 107). The ion-molecule reactor has been described elsewhere (Krechmer et al., 2018). The ion chemistry allows measurements of unsaturated hydrocarbons and functionalized species. Detection limits are 20 pptv for a 1-min integration. VOCs were identified according to nominal mass, context (i.e., outdoor, urban environment), and the literature (de Gouw & Warneke, 2007; Pagonis et al., 2019; Yuan et al., 2017). The investigators had limited access to the instrument because of the lockdown, compromising the data quality. Importantly, there is a period of two months between calibrations, and background measurements were only conducted after completion of the ambient measurements. These limitations are accounted for in our interpretation of the data. Further details about the work-up of the VOC data are given in Text S1 in Supporting Information S1.

Positive matrix factorization (PMF) was used for VOC source apportionment (Paatero, 1997; Paatero & Tapper, 1994). Briefly, PMF reconstructs the VOC data as factors, each consisting of a constant mass spectrum and a time series. The number of factors is chosen based on the interpretability of the solution (Ulbrich et al., 2009). This subjectivity as well as the sensitivities to additional parameters in the analysis are investigated using an ensemble of several PMF calculations.

In-situ measurements of NO, NO_2, O_3, CO, SO_2, $PM_{2.5}$ and PM_{10} were made at the CEMC site from 1 January until May 11, 2020. For historic perspective, we also obtained monitoring data for criteria pollutants from

six sites in Changzhou (see Figure S1 in Supporting Information S1 for locations). These data stop on May 23, 2020 defining the end of our post period.

For regional perspective, we use satellite data for NO_2 from the TROPOspheric Monitoring Instrument (TROPOMI) on the Sentinel 5-P satellite (Veefkind et al., 2012). NO_2 columns are shown in Figure S1 in Supporting Information S1 for each period of lockdown in 2020. Briefly, NO_2 columns are measured in the UV with a spatial resolution of 5.5×3.5 km^2. More details on data availability, selection and averaging are given in Text S2 in Supporting Information S1.

Meteorological data (2-m temperature, total precipitation; 1,000 mbar u and v wind components; boundary layer height) come from the European Centre for Medium-Range Weather Forecasts ERA5 reanalysis (ERA5, 2018; Hersbach et al., 2020).

3. Results and Discussion

3.1. Results of VOC Measurements

The total VOCs measured by the Vocus Elf (TVOCs) are presented in Figure 1 alongside average mass spectra for each period. Some species show strong responses to lockdown, representing possible tracers for emission sources, while others are less sensitive. We will exploit these differences for source attribution of VOCs using positive matrix factorization in Section 3.3, but first discuss observations for a few selected VOCs. Figure 1's box-plots summarize the concentrations during each level of lockdown for acetone, *N,N*-dimethylformamide (DMF), and toluene. These time periods are all statistically different for these three VOCs except for pre-lockdown and level 2 for toluene. Average diurnals are shown in Figure S4 in Supporting Information S1.

With fewer vehicles on the road during the lockdown, tailpipe emissions such as aromatics (e.g., benzene, toluene, C8-aromatics, and C9-aromatics observed in their protonated forms at *m/Q* 79, 93, 107, and 121, respectively) had reduced contributions to the TVOCs (Figure 1). However, not all aromatics responded in the same way: benzene, toluene, and C8-aromatics were reduced during level 1 by ~45%, ~67%, and ~76%, respectively (level 1 vs. pre-lockdown). These species have additional sources with variable emission ratios and responses to lockdowns, for example, volatile chemical products (VCPs). Furthermore, higher aromatics are removed faster by hydroxyl radicals and atmospheric aging adds uncertainties when considering larger-scale sources such as traffic.

DMF, observed in its protonated form at *m/Q* 74, is a solvent commonly used in the textile and pharmaceutical industries (H. Wang et al., 2021; Wang, Yuan, et al., 2020) and was reduced by ~54% during level 1. Ambient DMF concentrations in industrial zones sometimes surpass permitted workplace levels due to several local sources, although individual sources abide by emission regulations (H. Wang et al., 2021; Wei et al., 2011). The attribution of *m/Q* 74 to DMF was informed by mobile lab measurements using a similar, but higher mass resolution and higher sensitivity Vocus PTR-MS made near Changzhou. This data set will be described in greater detail elsewhere. Figure S5 in Supporting Information S1 shows mass spectra inside and outside a plume ~1 km downwind from a synthetic leather production facility on November 3, 2019 (~58 km SE of the CEMC site), and the time series for $C_3H_8NO^+$, the protonated molecular formula for DMF and other isomers, dominates the signal at *m/Q* 74 even outside the plume. DMF may serve as a reasonable tracer for these industries but is not a universal industrial tracer.

Acetone is both a primary emission, with evening enhancement during pre-lockdown, and a secondary product, as average nighttime and daytime concentrations are comparable as opposed to being diluted in the afternoon as observed with other species (Figure S4 in Supporting Information S1). Acetone was reduced by ~28% during level 1. Unlike DMF which is primarily used in industry, acetone is commonly used in VCPs such as paints, inks, and cleaners with significant indoor sources such as the home (McDonald et al., 2018). While industrial emissions of acetone may be reduced, VCP emissions were possibly less affected by lockdowns. Photochemical production further offsets the observed reductions in ambient concentrations.

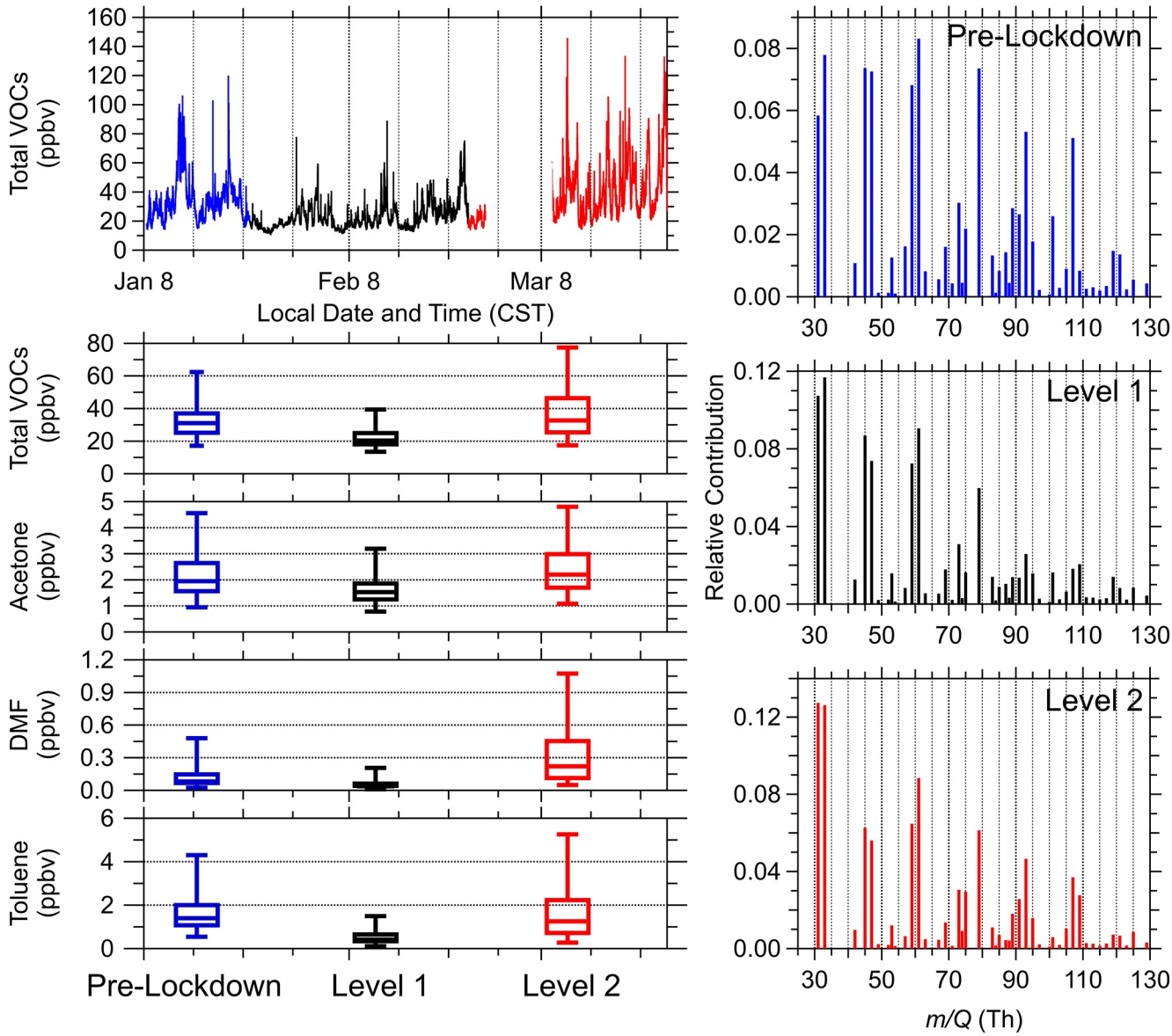

Figure 1. Time series for the total measured volatile organic compounds (VOCs) during the pre-lockdown (blue), level 1 (black), and level 2 (red) periods and their respective average mass spectra. Box-plots are also shown for total measured VOCs and a few select VOCs (whiskers are the 5th and 95th percentiles).

3.2. Observing and Defining Reductions in Concentrations During the Lockdowns

While these observed VOC reductions were seemingly large, several factors must be considered when inferring emission changes from observed ambient concentrations. Seasonal variability, differences in meteorology, long-term emission trends and the Chinese New Year celebrations can all lead to strong variability in observations (Bauwens et al., 2020; Goldberg et al., 2020). Due to the limitations of the VOC measurements, we use criteria pollutants to inform the VOC measurements.

We first consider the representativeness of our measurement site. The TROPOMI NO_2 columns over the Yangtze River Delta show widespread enhancements and were reduced over the entire urban corridor (Figure S1 in Supporting Information S1), agreeing with results shown elsewhere (Bauwens et al., 2020; Ding et al., 2020; Liu et al., 2020). In addition, in-situ measurements of criteria pollutants made at the CEMC site are consistent with those from six monitoring stations in Changzhou (locations in Figure S1 and

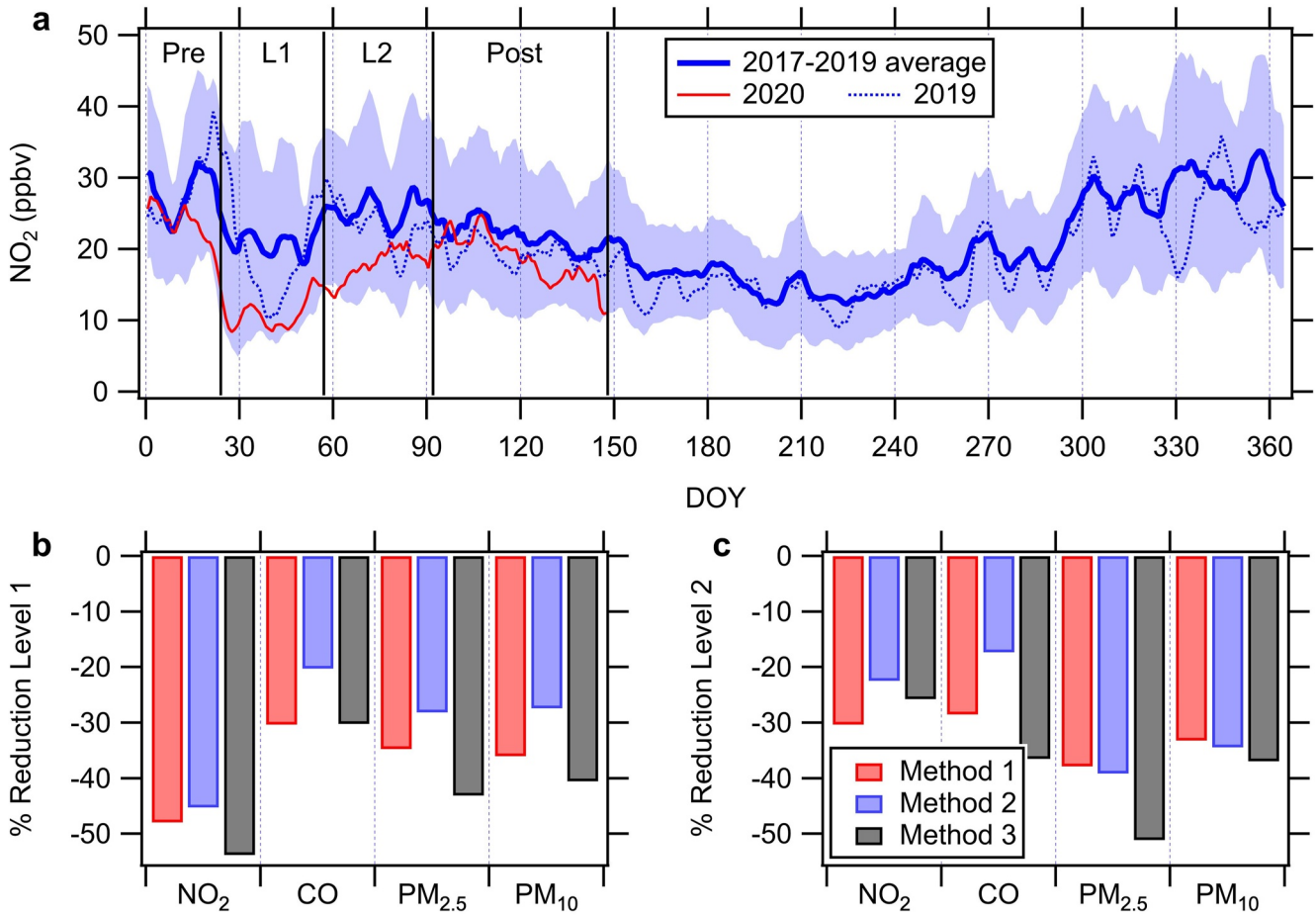

Figure 2. (a) Comparison between the in-situ NO_2 in 2020, 2019, and the 2017–2019 average. The data represent 7-day running means across 6 monitoring stations in Changzhou, with the shaded area showing the standard deviation in the 2017–2019 data. (b and c) Average reductions in measured concentrations during levels 1 and 2 using three methods: 2020 versus 2017–2019 average (method 1), 2020 versus 2019 (method 2), and the 2020 lockdown periods versus pre-lockdown (method 3).

measurements in Figures S6 and S7 in Supporting Information S1), indicating that measurements at the CEMC site are representative for the region.

We consider three methods to define our reductions. One method is to compare the 2020 lockdown period with the same period averaged over 2017–2019 (method 1). For pollutants with strongly decreasing emission trends like SO_2 in China, this method can overestimate the reductions caused by the lockdown. Another method compares against the same period in 2019 only (method 2) and is more susceptible to inter-annual differences. VOC data are only available for 2020, so the data obtained during level 1 and 2 are compared with the pre-lockdown period (method 3; used for acetone, DMF and toluene above). This method may overestimate the reductions resulting from the lockdowns because seasonal changes and the Chinese New Year also cause decreases in concentrations after January.

The VOC measurements are not extensive enough to make explicit corrections for meteorology. Our analysis indicates that temperature, boundary layer height, precipitation, and wind speed were not anomalous in 2020 relative to the 2017–2019 average. The level 1 wind direction had stronger North-West and South-East components in 2020. For the three cases, the boundary layer height increases from pre-lockdown to level 2 due to the transition into Spring (Figures S8–S11 in Supporting Information S1).

To further inform the VOC measurements, the three methods were compared using criteria pollutant measurements. Figure 2a shows the in-situ NO_2 for 2020, 2019 and the 2017–2019 average. In early January and throughout April, the 2020 data are close to the 2017–2019 average, but are reduced during the lockdown.

The 2019 data also show a significant decrease centered on DOY 40 due to the Chinese New Year holiday. However, the decrease in 2020 lasts longer and reflects the emissions reductions due to the lockdowns. Because this holiday is on a different calendar day each year, the 2017–2019 average data show a broader and shallower decrease.

The in-situ criteria air pollutant reductions are summarized in Table S2 in Supporting Information S1 and Figure 2b and generally agree with other observations made in the Yangtze River Delta (Li Li et al., 2020; Liu et al., 2020). In general, the three methods give similar results, suggesting that method 3 is a reasonable approximation. Method 2 gives smaller reductions than method 1 due to decreasing trends in air pollutant emissions. Method 3 overestimates the reductions relative to method 1 due to the seasonal cycle and Chinese New Year. This overestimation is by an average factor of 1.12 and 1.15 (average of NO_2, CO, $PM_{2.5}$, PM_{10}) during levels 1 and 2, respectively, and is incorporated into the uncertainties of the reported VOC reductions in the next section.

In summary, the observed relative reductions in VOC concentrations are assumed to reflect the relative reductions in emissions. We have established that the CEMC site reflects regional pollution beyond local sources. Additionally, the three methods for defining reductions during the lockdown agree for the criteria pollutants. The discrepancies between methods 1 and 3 are used to inform the uncertainties of the VOC reductions. These contributions to the uncertainties serve as corrections for differences in seasonal variation and meteorology during the different levels of lockdown.

3.3. Positive Matrix Factorization Analysis of VOC Data

VOC source apportionment was determined via PMF analysis, detailed in Text S3 in Supporting Information S1. A 7-factor solution was chosen as optimal, and a representative solution is shown in Figure 3. Additional factors improved the quality of fit (Figure S15 in Supporting Information S1) through factor splitting, which improves the overall fit, but does not add useful information. Fewer factors failed to describe all available data. Figure 3 shows the factors' profiles, time-series, and concentration distributions for each period, all of which are statistically different except for pre-lockdown and level 1 of the atmospheric background factor. Average diurnal variations are provided in Figures S19 and S20 in Supporting Information S1, and conditional probability wind rose plots are provided in Figure S21 in Supporting Information S1. Uncertainties are derived from the PMF sensitivity analysis, discussed later, and from the uncertainties and possible biases (seasonal variability and the Chinese New Year holiday) resulting from using the pre-lockdown data as the baseline (method 3; Table S2 in Supporting Information S1). We assume the primary emission factors originate from several point sources such that the observed reductions in factor concentrations correspond to an average emissions reduction for the source type.

Factors 1 and 2 are identified as industrial factors. Factor 1 is dominated by DMF and is attributed to the textile industry. Factor 2 is dominated by *m/Q* 73, attributed to protonated ions of tetrahydrofuran (THF) and methyl ethyl ketone (MEK), and *m/Q* 91, attributed to protonated butanediol isomers (BDO). THF and MEK are common reaction solvents in the pharmaceutical industry (Hu et al., 2018). BDO is a common raw material in drug manufacturing and is derived from various precursors (Busardò & Jones, 2015; Haas et al., 2005; Ji et al., 2011). We tentatively refer to this factor as the pharmaceutical industry factor, although it may represent several chemical industries. Relative to pre-lockdown, the textile and pharmaceutical industrial factors demonstrate reductions of 62 ± 10% and 40 ± 20%, respectively, during level 1 and enhancements of 150 ± 50% and 60 ± 50% during level 2. These different responses to lockdown highlight the need for caution when applying emission scaling factors to entire sectors.

The wind rose plots suggest several different sources (Figure S21 in Supporting Information S1) for both industries which were averaged into two representative PMF factors. Changzhou is a heavily industrialized city with dozens of pharmaceutical, textile, and chemical facilities which comprise large industrial parks, for example, the Changzhou National Hi-tech District to the North and Changfa Industrial Park to the South-East, and smaller industrialized zones scattered in and around Changzhou and neighboring cities. Both level 1 and pre-lockdown have strong North-West components. Level 2 has a strong South-East component, so different sources contributed to the measured VOCs compared to pre-lockdown and direct comparisons should be made with caution. In calculating average emission reductions, we assume each

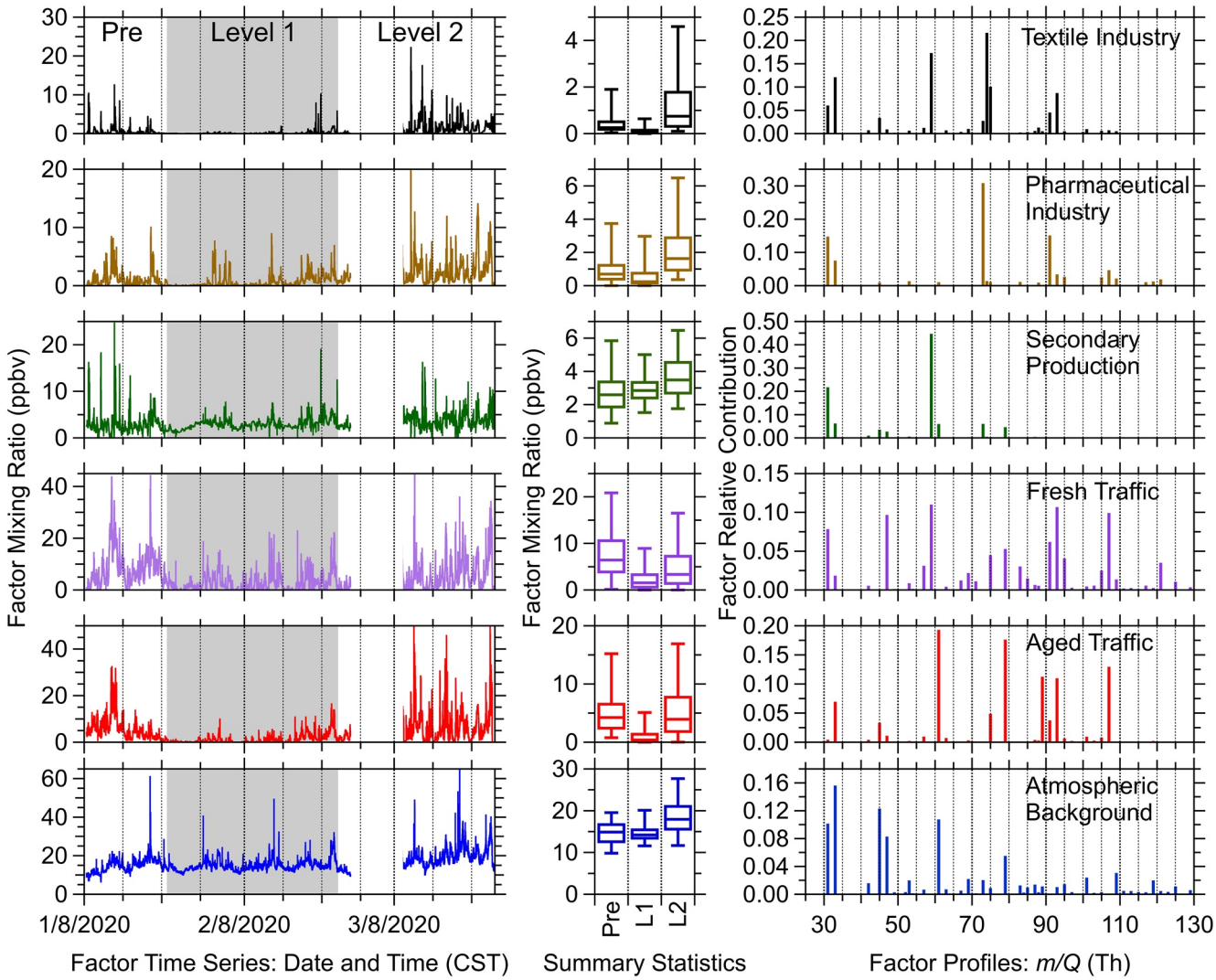

Figure 3. The factor time series, summary statistics (whiskers are the 5th and 95th percentiles), and profiles for a representative 7-factor positive matrix factorization solution. The atmospheric background factor is the sum of two factors of similar profile and anti-correlated in time.

period of lockdown has contributions from several emission sources which overall have a similar magnitude of emissions. The level 2 emission reductions have significantly greater uncertainties due to this shift in emission source.

Factor 3 is identified as a secondary production factor. Its profile is dominated by atmospheric oxidation products (e.g., acetone, formaldehyde, MEK, and acetic acid). These measurements took place during winter, so photochemistry is not strong. However, the average diurnal cycle demonstrates afternoon concentrations comparable to or exceeding evening concentrations, unlike the primary emissions factors which demonstrate reductions in the afternoon (Figure S19 in Supporting Information S1). With the transition to early Spring, this secondary factor shows a slightly stronger afternoon enhancement. Level 1 saw a 20 ± 20% reduction, possibly due to fewer precursors, while level 2 saw a 10 ± 40% enhancement, likely due to seasonal variations and recovery from lockdown.

Factors 4 and 5 are traffic-related due to their aromatic compositions: benzene, toluene, styrene, C8-aromatics, and C9-aromatics. Atmospheric reactions modify the composition of emissions, which may appear in PMF as a different factor (Yuan et al., 2012). Fresh vehicle emissions are rich in toluene and C8 aromatics, although their distributions vary with vehicle model, age, and fuel (Faber et al., 2013; Hong-li et al., 2017; Kumar et al., 2020). Aged traffic emissions have greater relative benzene contributions due to a higher

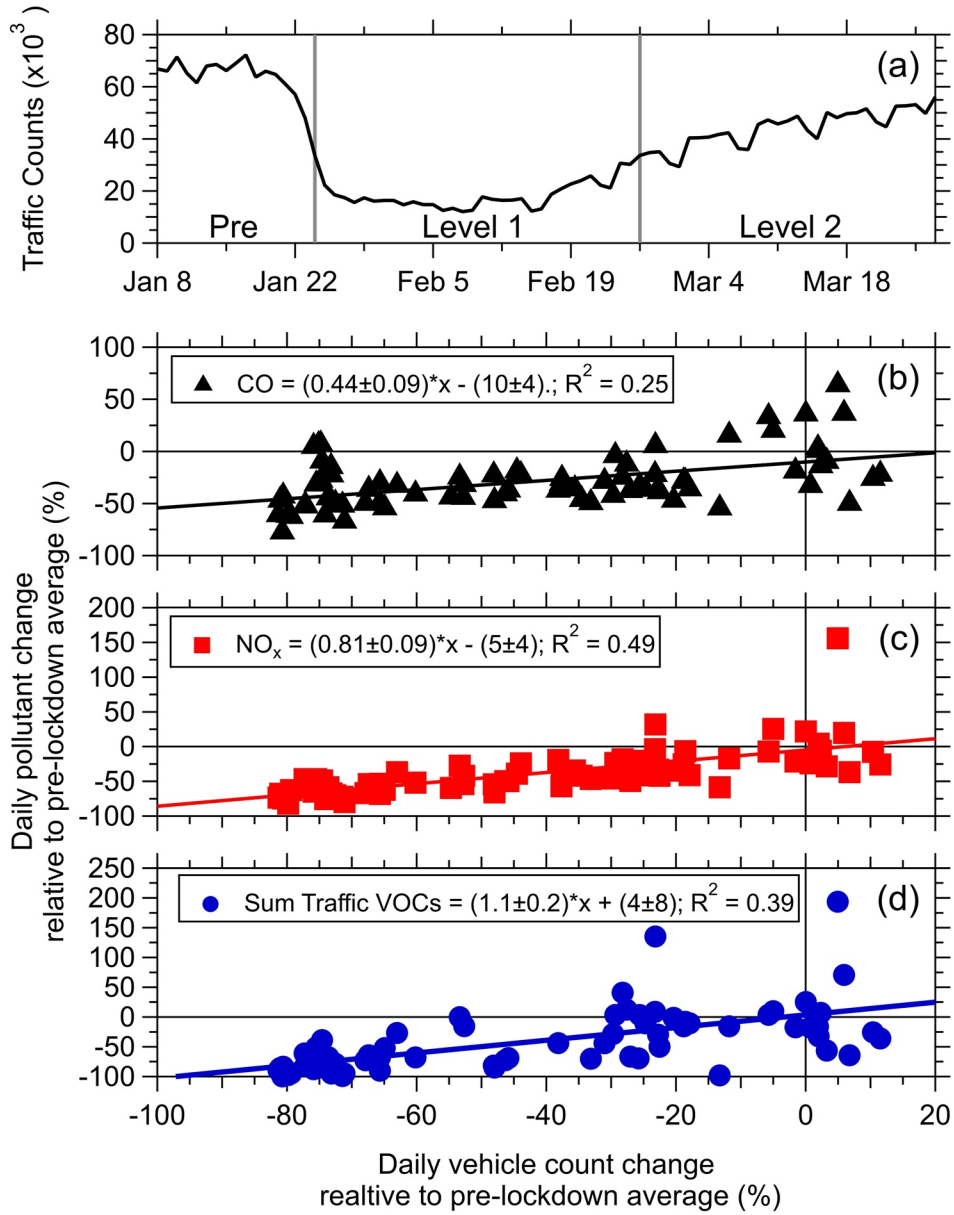

Figure 4. (a) Daily traffic counts collected at the intersection of Zhongwu Avenue and Heping Middle Road (31.753 N, 119.958 E; ~550 m from the Changzhou Environmental Monitoring Center site), and linear regressions of daily average concentration changes relative to the pre-lockdown average against the corresponding change in traffic counts for (b) CO, (c) NO_x, and (d) sum traffic volatile organic compounds.

degree of oxidation. The fresh and aged traffic factors are reduced during level 1 by 70 ± 11% and 73 ± 10%, respectively, consistent with the 71 ± 13% reduction in traffic counts (Figure 4a). The fresh traffic factor recovers during level 2, but is 30 ± 20% lower than pre-lockdown concentrations while the aged traffic factor is 10 ± 20% greater.

For the sum of both traffic factors, the daily average changes relative to the pre-lockdown average were regressed against the corresponding changes in vehicle counts near the measurement site (Figure 4d). Although atmospheric variability limits the strength of this correlation, the sum traffic factor is consistent with the traffic count. Within error, the complete removal of traffic corresponds to the complete removal of traffic-related VOCs such that vehicle counts are a sufficient proxy to estimate vehicle emissions of VOCs. A similar analysis of CO and NO_x shows a remaining contribution from these pollutants as traffic is completely removed (Fig-

ures 4b and 4c) due to additional non-traffic sources. CO also has a longer atmospheric lifetime such that an immediate reduction in emissions from vehicles does not yield the same immediate reduction in CO.

The "atmospheric background" factor primarily consists of oxygenated VOCs alongside longer-lived species. This factor is possibly affected by the imperfect determination of instrument backgrounds. Unresolved, low signal factors, for example, biogenic and biomass burning emissions, are likely encompassed by this factor. Tracers for biogenic emissions, for example, isoprene and monoterpenes, represented a small fraction of the total mass as the measurements were taken during winter months. These species were primarily attributed to the atmospheric background factor and were not resolved as a biogenic factor.

The presented case reconstructed on average (±1 SD), 98 ± 3% of the total mass. Of the 87 species, 6 species showed evidence of unresolved local sources and 8 species showed slow temporal changes which were not resolved for unknown reasons. Other PMF iterations are similar, although slightly variable depending on the resolved factors.

Sensitivities to PMF parameters and other aspects of data analysis (measurement errors, manual reweighting of species, minimum error correction, instrument background correction, calibration, and rotational ambiguity) were tested via an ensemble of 28 calculations (detailed in Text S3, Tables S3 and S4 in Supporting Information S1). All factors are relatively insensitive to perturbations in the estimated measurement errors and rotational ambiguity. The weights for some species were manually adjusted when the solution failed to capture the variability in that species or underwent factor splitting. Both traffic factors and the atmospheric background factor appear in all solutions of this subset with negligible variation as they are ubiquitous, while the industrial factors, which represents several individual sources, and secondary factor are more sensitive. The minimum error, instrument background correction, and calibration sensitivity studies led to the greatest uncertainties in all factors, although these perturbations are not wholly representative of the system. The sensitivity studies performed are not exhaustive and, while they provide an approximation of the uncertainties associated with lockdown reductions, they are likely underestimates. From all studies, the traffic factors and the atmospheric background factor are considered robust, the industrial factors were moderately robust, and secondary factor is most uncertain.

4. Conclusions

Following the outbreak of COVID-19, China underwent strict lockdowns in the interest of public health. These restrictions reduced the number of vehicles on the road, non-essential industrial productivity, and associated pollutant emissions. A PMF analysis of VOCs measured in Changzhou, China during these lockdowns resolved seven factors, with four of interest: two industries, traffic, and secondary chemistry. The textile and pharmaceutical industries had reduced emissions of 62 ± 10% and 40 ± 20%, respectively, during the strictest level of lockdown. These different responses highlight the need to address variability within sectors when modeling emissions. Traffic-related VOCs were reduced by 71 ± 10% in accordance with traffic counts. The influence of lockdown on secondary production of VOCs needs further investigation as the observed reduction, 20 ± 20%, is uncertain. These quantified reductions serve to constrain emission inventories, particularly for sectors where activity data are sparse, as the effects of lockdowns on air quality are explored.

Data Availability Statement

VOC and criteria pollutant data are publicly available on Open Science Framework (doi.org/10.17605/OSF.IO/4UG25). TROPOMI data are publicly available (NO_2: doi.org/10.5270/S5P-s4ljg54).

Acknowledgments
We acknowledge financial support from the CIRES Innovative Research Program. Li Li acknowledges support from the National Natural Science Foundation of China (NSFC project #42075144 and #41875161). This publication contains modified Copernicus Climate Change Service information (2020). Neither the European Commission nor ECMWF is responsible for any use that may be made of the Copernicus information or data it contains.

References

Bauwens, M., Compernolle, S., Stavrakou, T., Müller, J.-F., van Gent, J., Eskes, H., et al. (2020). Impact of coronavirus outbreak on NO_2 pollution assessed using TROPOMI and OMI observations. *Geophysical Research Letters*, *47*(11), e2020GL087978. https://doi.org/10.1029/2020GL087978

Busardò, F. P., & Jones, A. W. (2015). GHB pharmacology and toxicology: Acute intoxication, concentrations in blood and urine in forensic cases and treatment of the withdrawal syndrome. *Current Neuropharmacology*, *13*(1), 47–70. https://doi.org/10.2174/1570159X13666141210215423

Chang, Y., Huang, R.-J., Ge, X., Huang, X., Hu, J., Duan, Y., et al. (2020). Puzzling haze events in China during the coronavirus (COVID-19) shutdown. *Geophysical Research Letters*, *47*(12), e2020GL088533. https://doi.org/10.1029/2020GL088533

de Gouw, J., & Warneke, C. (2007). Measurements of volatile organic compounds in the earth's atmosphere using proton-transfer-reaction mass spectrometry. *Mass Spectrometry Reviews*, *26*(2), 223–257. https://doi.org/10.1002/mas.20119

Diffenbaugh, N. S., Field, C. B., Appel, E. A., Azevedo, I. L., Baldocchi, D. D., Burke, M., et al. (2020). The COVID-19 lockdowns: A window into the Earth System. *Nature Reviews Earth & Environment*, *1*(9), 470–481. https://doi.org/10.1038/s43017-020-0079-1

Ding, J., van der, A. R. J., Eskes, H. J., Mijling, B., Stavrakou, T., van Geffen, J. H. G. M., & Veefkind, J. P. (2020). NOx emissions reduction and rebound in china due to the COVID-19 crisis. *Geophysical Research Letters*, *47*(19), e2020GL089912. https://doi.org/10.1029/2020GL089912

ERA5. (2018). *Fifth generation of ECMWF atmospheric reanalyses of the global climate. Copernicus Climate Change Service Climate Data Store (CDS)*. https://doi.org/10.24381/cds.adbb2d47

Faber, J., Brodzik, K., Gołda-Kopek, A., & Łomankiewicz, D. (2013). Benzene, toluene and xylenes levels in new and used vehicles of the same model. *Journal of Environmental Sciences*, *25*(11), 2324–2330. https://doi.org/10.1016/S1001-0742(12)60333-7

Gkatzelis, G. I., Gilman, J. B., Brown, S. S., Eskes, H., Gomes, A. R., Lange, A. C., et al. (2021). The global impacts of COVID-19 lockdowns on urban air pollution: A critical review and recommendations. *Elementa: Science of the Anthropocene*, *9*(00176). https://doi.org/10.1525/elementa.2021.00176

Goldberg, D. L., Anenberg, S. C., Griffin, D., McLinden, C. A., Lu, Z., & Streets, D. G. (2020). Disentangling the Impact of the COVID-19 Lockdowns on Urban NO2 From Natural Variability. *Geophysical Research Letters*, *47*(17), e2020GL089269. https://doi.org/10.1029/2020GL089269

Guevara, M., Jorba, O., Soret, A., Petetin, H., Bowdalo, D., Serradell, K., et al. (2021). Time-resolved emission reductions for atmospheric chemistry modelling in Europe during the COVID-19 lockdowns. *Atmospheric Chemistry and Physics*, *21*(2), 773–797. https://doi.org/10.5194/acp-21-773-2021

Haas, T., Jaeger, B., Weber, R., Mitchell, S. F., & King, C. F. (2005). New diol processes: 1,3-propanediol and 1,4-butanediol. *Applied Catalysis A: General*, *280*(1), 83–88. https://doi.org/10.1016/j.apcata.2004.08.027

Hersbach, H., Bell, B., Berrisford, P., Hirahara, S., Horányi, A., Muñoz-Sabater, J., et al. (2020). The ERA5 global reanalysis. *Quarterly Journal of the Royal Meteorological Society*, *146*(730), 1999–2049. https://doi.org/10.1002/qj.3803

Hong-li, W., Sheng-ao, J., Sheng-rong, L., Qing-yao, H., Li, L., Shi-kang, T., et al. (2017). Volatile organic compounds (VOCs) source profiles of on-road vehicle emissions in China. *The Science of the Total Environment*, *607–608*, 253–261. https://doi.org/10.1016/j.scitotenv.2017.07.001

Hu, D., Li, X., Chen, Z., Cui, Y., Gu, F., Jia, F., et al. (2018). Performance and extracellular polymers substance analysis of a pilot scale anaerobic membrane bioreactor for treating tetrahydrofuran pharmaceutical wastewater at different HRTs. *Journal of Hazardous Materials*, *342*, 383–391. https://doi.org/10.1016/j.jhazmat.2017.08.028

Huang, X., Ding, A., Gao, J., Zheng, B., Zhou, D., Qi, X., et al. (2021). Enhanced secondary pollution offset reduction of primary emissions during COVID-19 lockdown in China. *National Science Review*, *8*(2), nwaa137. https://doi.org/10.1093/nsr/nwaa137

Ji, X.-J., Huang, H., & Ouyang, P.-K. (2011). Microbial 2,3-butanediol production: A state-of-the-art review. *Biotechnology Advances*, *29*(3), 351–364. https://doi.org/10.1016/j.biotechadv.2011.01.007

Krechmer, J., Lopez-Hilfiker, F., Koss, A., Hutterli, M., Stoermer, C., Deming, B., et al. (2018). Evaluation of a new reagent-ion source and focusing ion–molecule reactor for use in proton-transfer-reaction mass spectrometry. *Analytical Chemistry*, *90*(20), 12011–12018. https://doi.org/10.1021/acs.analchem.8b02641

Kroll, J. H., Heald, C. L., Cappa, C. D., Farmer, D. K., Fry, J. L., Murphy, J. G., & Steiner, A. L. (2020). The complex chemical effects of COVID-19 shutdowns on air quality. *Nature Chemistry*, *12*(9), 777–779. https://doi.org/10.1038/s41557-020-0535-z

Kumar, A., Sinha, V., Shabin, M., Hakkim, H., Bonsang, B., & Gros, V. (2020). Non-methane hydrocarbon (NMHC) fingerprints of major urban and agricultural emission sources for use in source apportionment studies. *Atmospheric Chemistry and Physics*, *20*(20), 12133–12152. https://doi.org/10.5194/acp-20-12133-2020

Le, T., Wang, Y., Liu, L., Yang, J., Yung, Y. L., Li, G., & Seinfeld, J. H. (2020). Unexpected air pollution with marked emission reductions during the COVID-19 outbreak in China. *Science*, *369*(6504), 702–706. https://doi.org/10.1126/science.abb7431

Li, L., Li, Q., Huang, L., Wang, Q., Zhu, A., Xu, J., et al. (2020). Air quality changes during the COVID-19 lockdown over the Yangtze River Delta Region: An insight into the impact of human activity pattern changes on air pollution variation. *The Science of the Total Environment*, *732*, 139282. https://doi.org/10.1016/j.scitotenv.2020.139282

Li, L., Hu, J., Li, J., Gong, K., Wang, X., Ying, Q., et al. (2021). Modelling air quality during the EXPLORE-YRD campaign–Part II. Regional source apportionment of ozone and PM2.5. *Atmospheric Environment*, *247*, 118063. https://doi.org/10.1016/j.atmosenv.2020.118063

Liu, F., Page, A., Strode, S. A., Yoshida, Y., Choi, S., Zheng, B., et al. (2020). Abrupt decline in tropospheric nitrogen dioxide over China after the outbreak of COVID-19. *Science Advances*, *6*, eabc2992. https://doi.org/10.1126/sciadv.abc2992

Mahato, S., Pal, S., & Ghosh, K. G. (2020). Effect of lockdown amid COVID-19 pandemic on air quality of the megacity Delhi, India. *The Science of the Total Environment*, *730*, 139086. https://doi.org/10.1016/j.scitotenv.2020.139086

McDonald, B. C., de Gouw, J. A., Gilman, J. B., Jathar, S. H., Akherati, A., Cappa, C. D., et al. (2018). Volatile chemical products emerging as largest petrochemical source of urban organic emissions. *Science*, *359*(6377), 760–764. https://doi.org/10.1126/science.aaq0524

Paatero, P. (1997). Least squares formulation of robust non-negative factor analysis. *Chemometrics and Intelligent Laboratory Systems*, *37*(1), 23–35. https://doi.org/10.1016/S0169-7439(96)00044-5

Paatero, P., & Tapper, U. (1994). Positive matrix factorization: A non-negative factor model with optimal utilization of error estimates of data values. *Environmetrics*, *5*(2), 111–126. https://doi.org/10.1002/env.3170050203

Pagonis, D., Sekimoto, K., & de Gouw, J. (2019). A library of proton-transfer reactions of H_3O^+ ions used for trace gas detection. *Journal of the American Society for Mass Spectrometry*, *30*(7), 1330–1335. https://doi.org/10.1007/s13361-019-02209-3

Shi, X., & Brasseur, G. P. (2020). The response in air quality to the reduction of Chinese economic activities during the COVID-19 Outbreak. *Geophysical Research Letters*, *47*(11), e2020GL088070. https://doi.org/10.1029/2020GL088070

Singh, R. P., & Chauhan, A. (2020). Impact of lockdown on air quality in India during COVID-19 pandemic. *Air Quality, Atmosphere & Health*, *13*(8), 921–928. https://doi.org/10.1007/s11869-020-00863-1

Tanzer-Gruener, R., Li, J., Eilenberg, S. R., Robinson, A. L., & Presto, A. A. (2020). Impacts of modifiable factors on ambient air pollution: A case study of COVID-19 shutdowns. *Environmental Science and Technology Letters*, *7*(8), 554–559. https://doi.org/10.1021/acs.estlett.0c00365

Ulbrich, I. M., Canagaratna, M. R., Zhang, Q., Worsnop, D. R., & Jimenez, J. L. (2009). Interpretation of organic components from Positive Matrix Factorization of aerosol mass spectrometric data. *Atmospheric Chemistry and Physics*, *9*(9), 2891–2918. https://doi.org/10.5194/acp-9-2891-2009

Veefkind, J. P., Aben, I., McMullan, K., Förster, H., de Vries, J., Otter, G., et al. (2012). TROPOMI on the ESA Sentinel-5 Precursor: A GMES mission for global observations of the atmospheric composition for climate, air quality and ozone layer applications. *Remote Sensing of Environment*, *120*, 70–83. https://doi.org/10.1016/j.rse.2011.09.027

Wang, H., Gao, Y., Jing, S., Lou, S., Hu, Q., An, J., et al. (2021). Characteristics of volatile organic compounds pollution in the atmosphere around the Yangtze River Delta Industrial park based on navigation monitoring. *Environmental Sciences*, *42*(3), 1298–1305. https://doi.org/10.13227/j.hjkx.202007265

Wang, P., Chen, K., Zhu, S., Wang, P., & Zhang, H. (2020). Severe air pollution events not avoided by reduced anthropogenic activities during COVID-19 outbreak. *Resources, Conservation and Recycling*, *158*, 104814. https://doi.org/10.1016/j.resconrec.2020.104814

Wang, Z., Yuan, B., Ye, C., Roberts, J., Wisthaler, A., Lin, Y., et al. (2020). High Concentrations of Atmospheric Isocyanic Acid (HNCO) produced from secondary sources in China. *Environmental Science & Technology*, *54*(19), 11818–11826. https://doi.org/10.1021/acs.est.0c02843

Wei, Y., Tian, W., Zheng, Y., Zhang, Q., Jiang, L., & Wu, Z. (2011). Modelling of urban ambient N, N-dimethylformamide concentrations in a small-scale synthetic leather industrial zone. *Journal of Zhejiang University Science A*, *12*(5), 374–389. https://doi.org/10.1631/jzus.A1010245

Yuan, B., Koss, A. R., Warneke, C., Coggon, M., Sekimoto, K., & de Gouw, J. A. (2017). Proton-Transfer-reaction mass spectrometry: Applications in atmospheric sciences. *Chemical Reviews*, *117*(21), 13187–13229. https://doi.org/10.1021/acs.chemrev.7b00325

Yuan, B., Shao, M., de Gouw, J., Parrish, D. D., Lu, S., Wang, M., et al. (2012). Volatile organic compounds (VOCs) in urban air: How chemistry affects the interpretation of positive matrix factorization (PMF) analysis. *Journal of Geophysical Research: Atmospheres*, *117*(D24), D24302. https://doi.org/10.1029/2012JD018236

References From the Supporting Information

Cappellin, L., Karl, T., Probst, M., Ismailova, O., Winkler, P. M., Soukoulis, C., et al. (2012). On quantitative determination of volatile organic compound concentrations using proton transfer reaction time-of-flight mass spectrometry. *Environmental Science & Technology*, *46*(4), 2283–2290. https://doi.org/10.1021/es203985t

Isokääntä, S., Kari, E., Buchholz, A., Hao, L., Schobesberger, S., Virtanen, A., & Mikkonen, S. (2020). Comparison of dimension reduction techniques in the analysis of mass spectrometry data. *Atmospheric Measurement Techniques*, *13*(6), 2995–3022. https://doi.org/10.5194/amt-13-2995-2020

Paatero, P., & Hopke, P. K. (2003). Discarding or downweighting high-noise variables in factor analytic models. *Analytica Chimica Acta*, *490*(1), 277–289. https://doi.org/10.1016/S0003-2670(02)01643-4

Sekimoto, K., Li, S.-M., Yuan, B., Koss, A., Coggon, M., Warneke, C., & de Gouw, J. (2017). Calculation of the sensitivity of proton-transfer-reaction mass spectrometry (PTR-MS) for organic trace gases using molecular properties. *International Journal of Mass Spectrometry*, *421*, 71–94. https://doi.org/10.1016/j.ijms.2017.04.006